A national laboratory of the U.S. Department of Energy
Office of Energy Efficiency & Renewable Energy

National Renewable Energy Laboratory

*Innovation for Our Energy Future*

# The Great Plains Turbulence Environment: Its Origins, Impact and Simulation

N.D. Kelley, B.J. Jonkman, and G.N. Scott
*National Renewable Energy Laboratory*

*Presented at AWEA's 2006 WindPower Conference*
*Pittsburgh, Pennsylvania*
*June 4–7, 2006*

***Conference Paper***
**NREL/CP-500-40176**
**December 2006**

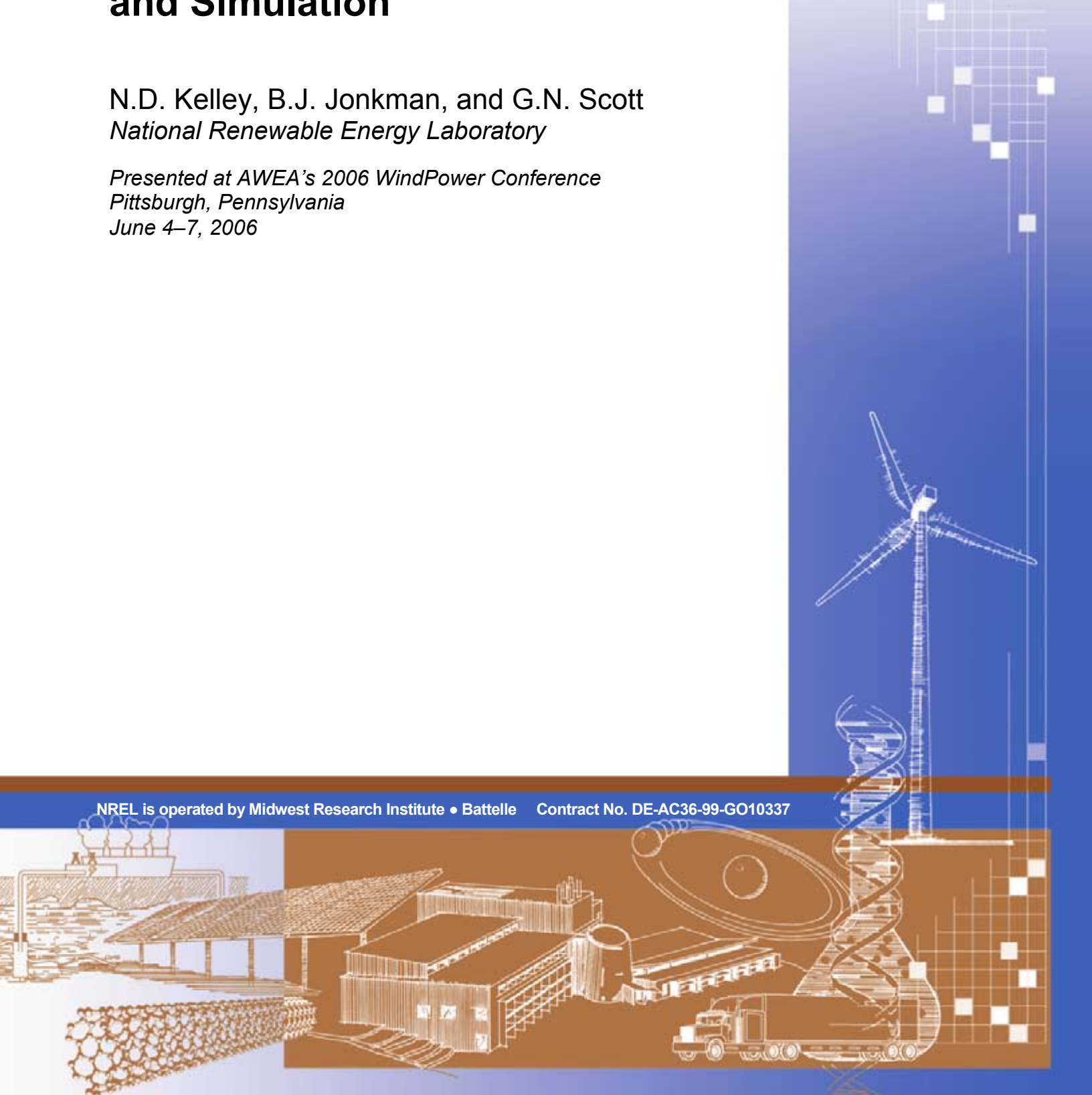

NREL is operated by Midwest Research Institute • Battelle Contract No. DE-AC36-99-GO10337

# The Great Plains Turbulence Environment: Its Origins, Impact, and Simulation

**Neil D. Kelley, Bonnie J. Jonkman, and George N. Scott**
*National Wind Technology Center*
*National Renewable Energy Laboratory*
*Golden, Colorado 80401*

## Abstract

Research conducted over the past 15 years has demonstrated that organized or coherent turbulence structures in turbine inflows are often responsible for increased structural loading and fatigue damage as well as the loss of availability during turbine operations. Turbine heights and dimensions, including the turbine design, siting, and operations, continue to increase. Thus, the role of site specificity of the turbulent inflow environment, particularly at night, has become very important in all phases of wind plant development including the turbine design, siting, and operations. In this paper we summarize the known impacts of nocturnal turbulence on wind turbine performance and operations. We discuss our progress in numerically simulated coherent inflow turbulent conditions generated by atmospheric instabilities that are frequently associated with a Great Plains nocturnal low-level jet stream. Finally, we compare the general characteristics of nocturnal turbulent flows that are associated with wind farms in or near complex terrain with those installed over more homogenous landforms but in the presence of low-level jet streams.

## Introduction

The Great Plains, particularly its western extent, is the largest region of high wind resource in the United States. It is characterized by frequent, strong, high-level winds during the nighttime hours. The same region has frequent flows of more energetic winds, called *low-level jet streams* (LLJs), that form in the lowest 500 m above the ground, particularly at night. These LLJs are often responsible for the substantially greater wind resource associated with increasing height that is characteristic of the Great Plains. The availability of this resource is driving wind turbine designs to ever-increasing hub heights and rotor diameters. To capture a better resource in more numerous but less energetic wind regimes closer to population centers, the Low-Wind Speed Turbine (LWST) Project of the U.S. Department of Energy (DOE) envisions taking advantage of stronger winds that frequently occur at higher altitudes in such areas by looking at turbine designs with nameplate capacities as large as (and possibly larger than) 5 MW. Such designs will necessitate larger diameter rotors that operate farther from the ground and extend deeper into the atmospheric boundary layer.

## Background

The wind energy technologies that can take advantage of increased wind speeds at higher altitudes require larger diameter rotors that rise deeper into the atmospheric boundary layer. These rotors and the large support structures necessary to support them have been accompanied by an increase in structural flexibility that is often further exacerbated by the need to reduce weight. The result has been that the large turbines currently being installed are also more

dynamically active. In [1] we discussed the potential role of nocturnal LLJs that are prevalent in the areas targeted for potential LWST installations such as the Great Plains. In [2] we discussed that, although nocturnal LLJs provide the benefit of an increased wind resource with height, they also supply the intense vertical wind shears and temperature gradients below the height of the LLJ maximum velocities that feed the development of atmospheric instabilities such as Kelvin-Helmholtz Instability (KHI). As discussed in both [1] and [2], KHI is responsible for creating intense bursts of coherent turbulence in the nighttime (statically stable) boundary layer. During the day, the boundary layer is usually statically *unstable* or *convective* and will not support KHI. Convective motions typically have spatial dimensions that are much larger than the largest wind turbine, whereas coherent motions associated with KHI in a stable boundary layer can be the same size as the largest turbine rotors or much smaller. KHI occurs when the vertical gradients of temperature and wind speed allow atmospheric wave motions called *billows* or KH waves to develop. The KH billows actually represent a form of *atmospheric resonance* in the turbulent wind field that is controlled by stability (vertical motions being *damped* by negative buoyancy).

In [2] we reviewed our research in determining the role of coherent or organized turbulence in the aeroelastic and structural response of wind turbines. We found, for example, that the severity of structural loads generated by the turbine rotor passing through coherent turbulence can be scaled by knowledge of the vertical stability of the layer of air above the ground within which the turbine resides, a fluid dynamic property that represents the *intensity* (not turbulence intensity!) of the turbulence, and the standard deviation of the vertical wind speed measured within the rotor disk.

We determine the turbine layer vertical stability by the dimensionless *gradient Richardson number*:

$$Ri_g = (g/\overline{T})(\Delta T/\Delta z)/(\Delta U/\Delta z)^2 \qquad (1)$$

where

$g$ = the gravity acceleration
$T$ = the absolute air temperature
$U$ = the wind speed
$Z$ = the height above the ground.

Equation (1) represents the ratio of turbulence generation by vertical temperature (density) differences or buoyancy in the numerator to that by wind shear (the rate of change of wind speed with height) in the denominator. A negative value of $Ri_g$ corresponds to *unstable* flow conditions within the layer from the surface to the top of the turbine rotor (what we refer to as the *turbine layer*), a positive value corresponds to *stable* conditions, and zero neutral. In unstable flows ($Ri_g < 0$) vertical temperature differences with height (*positive buoyancy or convection*) add kinetic energy to the turbulence while in stable ($Ri_g > 0$) ones, energy is removed (*negative buoyancy damping*). Neutral conditions ($Ri_g = 0$) represent a flow in which turbulence is being generated only through the action of wind shear; buoyancy has no influence. Neutrally stable flows are of theoretical interest because of the simplifications they allow, but the condition is infrequent in the real atmosphere (or at least in the portion of the atmosphere occupied by wind turbines). For

example, in our recent experiment in Lamar, Colorado, true neutral conditions in the layer 3−116 m above ground level (AGL) were observed on only 14 out of 4,676 hours of record or less than 0.3% of the time.

As an illustration, Figure 1 plots the damage equivalent loads (DELs) measured at the root of one of the blades of the Advanced Wind Turbine (ART) at the National Wind Technology Center (NWTC). The highest loads occur within a small range of just slightly positive or *weakly stable* values of $Ri_g$ between 0 and +0.1. Similar results have often been observed at other sites and with other turbine designs.

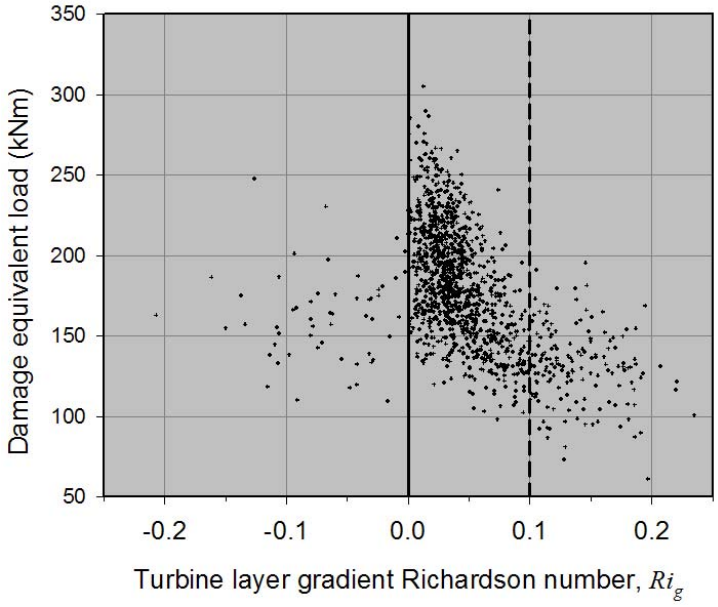


**Figure 1. The observed variation in the damage equivalent blade root load seen on the NWTC ART as a function of atmospheric stability expressed by the turbine layer gradient Richardson number, $Ri_g$.**

The intensity of the *coherent* turbulence as measured by a property of the flow that we have defined as the *coherent turbulent kinetic energy* or CTKE and is expressed as

$$\mathrm{CTKE} = 1/2[(u'w')^2 + (u'v')^2 + (v'w')^2]^{1/2} \quad [\mathrm{m}^2/\mathrm{s}^2] \qquad (2)$$

where *u'*, *v'*, and *w'* are the instantaneous fluctuating streamwise, lateral or crosswind, and vertical wind velocity components (with the mean values removed). Finally we represent the standard deviation of the vertical wind component as $\sigma_w$. All these variables play important roles in KHI.

## The Need for Site-Specific Information in Turbine Design

As the size of turbines has continued to increase the demands to reduce weight, and particularly the weight at the top of the tower, the need to use lighter and stronger materials has become acute. The combination of lighter materials and the shear size of the newest turbines have led to machines that are now much more dynamically active than their smaller and less flexible predecessors. For example, a linear frequency analysis of the NWTC 600 kW ART turbine found 12 static vibrational modes ranging from 0.03 to 10.8 Hz up to a maximum of 15 Hz. A similar analysis of a fictitious 1.5-MW design developed by Malcolm and Hansen [3] for the DOE Wind Partnership for Advanced Component Technologies (WindPACT) turbine rotor design study exhibited 31 modes ranging from 0.4 to 20.4 Hz up to a maximum of 20.4 Hz. Jonkman, et al. [4] recently developed a 5-MW virtual baseline turbine design that will be used primarily for offshore studies. This design encompasses 52 static modes in the frequency range of 0.32 to 19.84 Hz up to 20 Hz. The actual number of participating modal frequencies is even

greater when nonlinear and rotational modes are considered. The message is that these larger designs may be more susceptible to turbulent inflow characteristics because their rotors are operating throughout a larger atmospheric depth and whose dynamic response includes the contributions of an increasing number of active vibrational modes, raising the possibility both of nonlinear interactions between them and of dynamic amplification. There is some evidence available in the public domain, albeit sketchy, that this is occurring.

## Design Criteria

Current design practice depends heavily on inflow conditions specified by the International Electrotechnical Commission (IEC) in its third edition of the consensus-derived IEC 61400-1 design standard [5]. Page 7 of this document specifies that it "outlines design requirements for wind turbines and is not intended for use of a complete design specification or instruction manual." The standard is primarily aimed toward ensuring turbine operating safety and survivability with the required series of discrete loading conditions generally associated with severe operating events that have occurrences with one- and 50-year return cycles. "Normal" operating conditions are specified via a vertical shear expressed by a power law variation across the rotor disk with a shear exponent of 0.2 (the Normal Wind Profile or NWP) and the user's choice of two recommended turbulence models for a neutrally stable atmosphere. The velocity spectrum is scaled by a turbulence level that is based on the 90th percentile of the observed standard deviation of the streamwise wind component ($u$) defined in terms of one of three severity classes that have expected values of turbulence intensities of 12%, 14%, and 16%. A model is provided for spatial correlation or coherence in only the streamwise ($u$) wind component. In the case of the IEC Kaimal [6] Normal Turbulence Model (NTM) the velocities at all points within the rotor disk are scaled uniformly. The only variation occurs in the streamwise component when the spatial coherence model is applied. The IEC version of the Mann [7,8] uniform shear turbulence model generates a turbulence spectrum that redistributes initially the equal amount of kinetic energy in each of the three wind components from the vertical ($w$) to the streamwise ($u$), and crosswind ($v$) components as the result of a uniform mean shear. In both models the velocity fields produced are assumed to be stationary with zero-mean Gaussian statistics. The idealized IEC inflow and turbulence models are meant as a reference for load calculation comparisons and do not reflect any particular specific operating environment. It is the responsibility of the designer to identify and include any site specific inflow conditions and the loads resulting from them that may exceed IEC criteria through the use of the "Special Class" category.

## Actual Turbulent Inflow and Its Consequences

Boundary layer flows in the real atmosphere have properties that often differ considerably from those outlined by the IEC criteria. We previously discussed the role of coherent, nonisotropic and nonstationary turbulent inflows on the dynamic response of wind turbine rotors and structural components [9]. In this paper we demonstrated that the increased fatigue damage seen on turbines during the nighttime hours is largely the result of operating in coherent turbulence that develops in the stable atmospheric boundary layer. Intense vertical wind shear and temperature gradients create resonant flow fields that can impart short-period loading and vibrational energy as wind turbine rotor blades pass through regions of organized or coherent

turbulence. This energy is subsequently propagated throughout the remainder of the structure, where it is likely to be dissipated locally. Such conditions cannot be reproduced well, or perhaps not at all, with the inflow as defined by the IEC NTM, although some of the specified discrete loading events are as intense (or even more so) than those seen in the real atmosphere. The problem occurs when these high shear and coherent flow conditions occur with significant frequency. If a turbine design is not evaluated with simulations of such inflows and the loads created occasionally exceed IEC criteria, problems may result when the turbine is installed in a location with flows that exhibit such characteristics.

## Site-Specific Inflow Simulations

We have used the results of three major field experiments to develop site-specific inflow simulations that replicate the characteristics of inflows found:

- Upwind, within, and downwind of a large wind park that consists of small (by today's standards) turbines with generating capacities of 44 to 105 kW
- Downwind of complex terrain (the NWTC)
- At a site in the Great Plains (Lamar, Colorado) with and without the presence of a nocturnal LLJ.

The most extensive set of data is available for the latter two sites, so we focused our efforts based on them. Although we have found that coherent structures are consistent features of nocturnal flows at all three locations, we have more information about them from data collected at the NWTC and the high plains south of Lamar.

## Known Impacts of Nocturnal Flows in the Great Plains

Unfortunately, we do not have access to a large body of information that summarizes turbine operational problems in various locations in the Great Plains, as it is proprietary. Smith et al. [10] analyzed an extensive set of data collected from the long-term monitoring of a wind farm in Texas, in which they found that the diurnal variation of number of hours with turbines in a faulted condition began to increase just before midnight, reached a peak just before sunrise, and then declined and remained relatively low until a slight rise began again about mid-afternoon. They also found that the mean wind shear closely followed the trend in fault frequencies but began rising late in the afternoon reaching a broad peak between midnight and sunrise before decreasing in a similar manner as the fault data. These results suggest a decent correlation between conditions seen in the nocturnal boundary layer and the operational experience of a large wind farm.

We were fortunate to have access to a small number of operations data from a wind farm in the northern Great Plains taken during the month of August. A number of fault categories were analyzed diurnally for the month. Figure 2a plots the mean hub-height wind speeds and shear exponent measured from the bottom of the rotor to the height of the nacelle for each hour starting at 18:00 local time. The shear exponent exceeds the IEC value of 0.2 until 10:00 and remains below that value until 17:00. The mean wind speeds are slightly higher during the nighttime

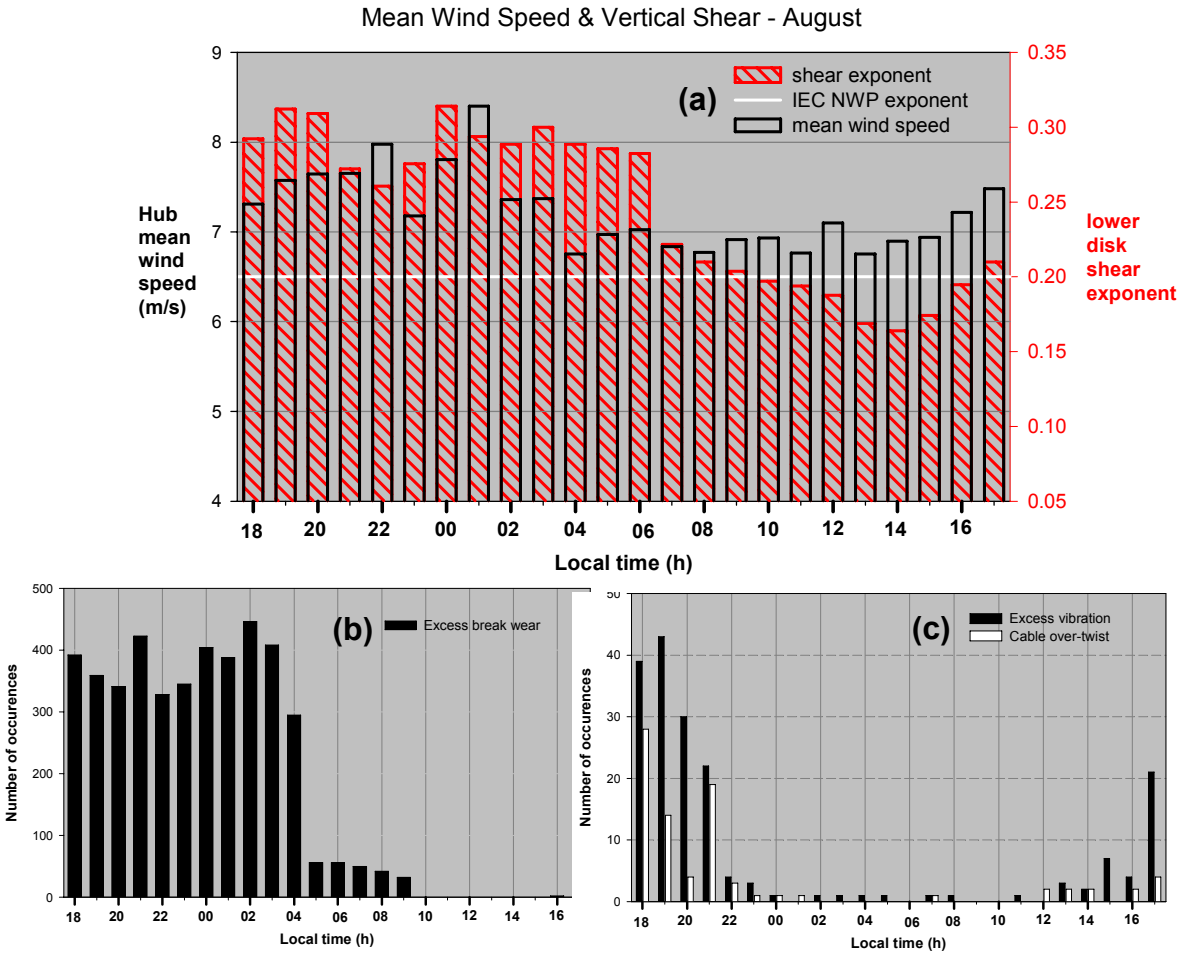


**Figure 2. Example of correlation between diurnal wind conditions and turbine fault history: (a) hourly average wind speed and shear, (b) excessive break wear fault frequency, (c) excessive vibration and cable over-twist fault frequencies.**

hours. The number of excessive brake wear faults that occurred for the month is plotted by the hour in Figure 2b, and again the correlation with the periods of high shear is quite good, suggesting that there may be a cause and effect. The number of hours in which there was either an excessive vibration or cable-over-twist fault are plotted in Figure 2c. It shows that excessive vibration faults are common starting about mid-afternoon and reach a peak about 19:00. The cable-over-twist plot shows fewer faults but a similar occurrence pattern. Between 16:00 and 23:00 the boundary layer transitions from a daytime convective regime to a nocturnal stable characteristic. Several turbulent processes take place during this period and may influence the generation of these faults. We will discuss these processes more fully later.

## Coherent Turbulence Conditions in the Great Plains

The Great Plains provide an excellent wind resource but are also home to atmospheric phenomena that can produce occasional intense coherent turbulent activity. Severe local storms can generate gust fronts, microbursts, and tornadic winds. These, fortunately, are seasonal for a

specific location and generally occur infrequently; however, some regions have a higher probability than others. The U.S. National Severe Storms Laboratory calculates that the probability of experiencing a tornado on a given day in the vicinity of Lamar, Colorado, is 1.2% during May and June but essentially zero in December. The probability of experiencing a severe thunderstorm gust faster than 26 m/s (58 mph) is slightly higher at 1.4% in May-June but less than 0.05% in December. We analyzed the year-long record of nocturnal turbulence measurements collected between 16:00 and 08:00 LST from the GE Wind 120-m tower south of Lamar to establish the probabilities of encountering two intensity levels of coherent turbulent structures. Experience has shown that structures that contain peak CTKE intensities of at least 2 $m^2s^{-2}$ are sufficient to induce a noticeable structural response in an operating wind turbine. Structures that contain peak CTKE values 10 $m^2s^{-2}$ or higher may be considered *intense* and are capable of inducing a *significant* turbine structural response. Our analysis of the available period between March 2002 and March 2003 found the probability of a turbine rotor encountering a coherent structure between the hours of 16:00 and 08:00 LST with CTKE intensities 2 $m^2s^{-2}$ or greater during May and June is 52% in May and June and 6% in December. The probability of ingesting an intense structure is 6% and 0.2% during those respective periods. Thus, at the Lamar site turbines are exposed to turbulent coherent structures related to instabilities in the nocturnal boundary layer far more often than those accompanying a severe thunderstorm or even a tornado.

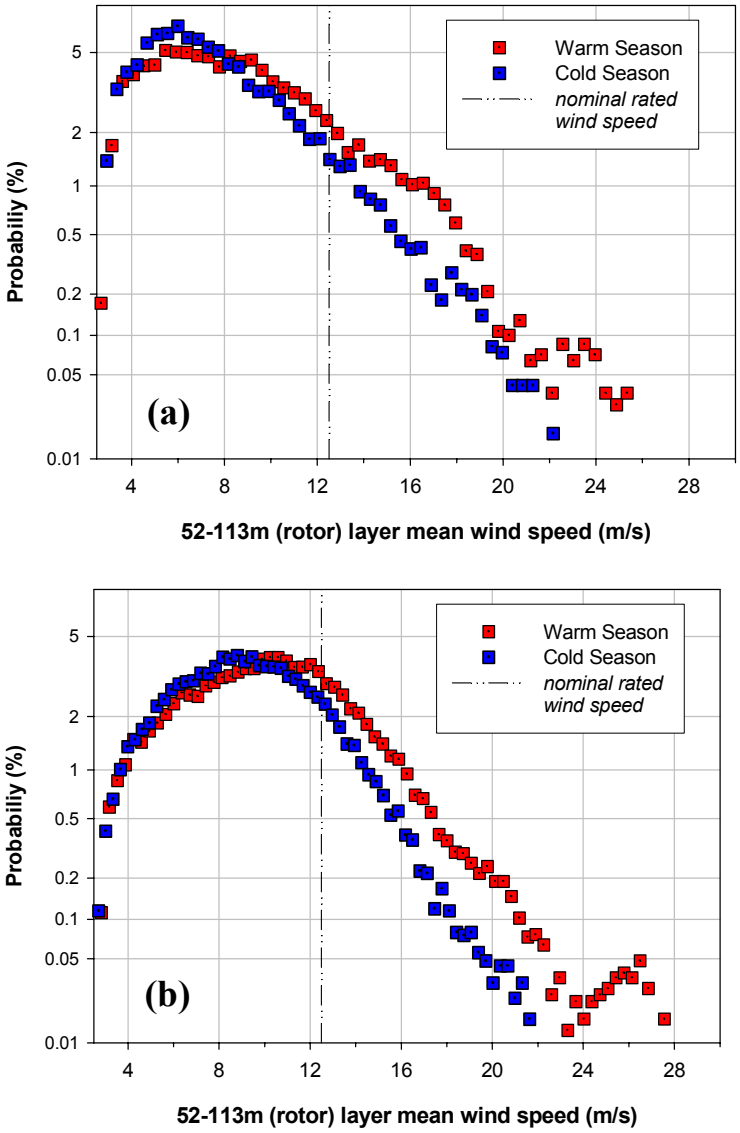


**Figure 3. Annual probability distributions of the 52−113m layer mean wind speed for the Lamar Site: (a) 08:00 to 16:00 LST, (b) 16:00 to 08:00 LST.**

Mitchell et al. [11] and Whiteman et al. [12] found two distinct seasons for LLJ formation. Jets during the "Warm Season" (April-September) are more frequently associated with southerly winds and are *more persistent* and *intense* with the height of their *wind speed maximums nearer to the ground*. From October through March (the "Cold Season"), LLJs are more transient, less intense, and often associated with the northerly winds behind passing cold fronts. We found for the Lamar site that the wind resource is better during the nocturnal hours in both the warm and cold jet seasons. The probability plots of the mean wind speed for the 52- to 113-m layer that are shown in Figure 3 demonstrate this. Monthly distributions of the probability of coherent structure intensities are presented in Figure 4. Clearly the warm season months have a greater probability of coherent structures, including the more intense ones. The probabilities shown during the months of July and August 2002 may be lower than would normally be expected because of the severe drought and the very stable and hot atmosphere present during that period of time.

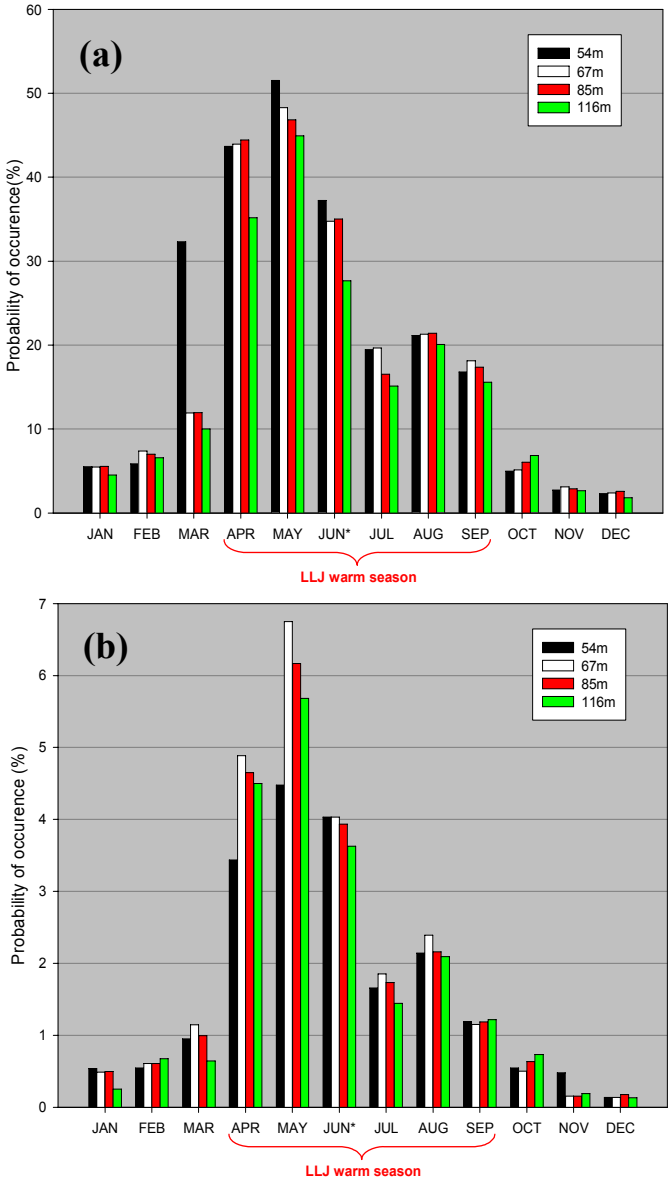


**Figure 4. Probability distributions of: (a) coherent turbulent events with intensities of $2 m^2/s^2$ or greater, (b) intensities 10 $m^2/s^2$ or greater. *(*June was limited to range of 19:00 to 05:00 LST because of an undetected instrumentation problem)***

## Progress in Simulating Great Plains Turbulent Inflows

We have recently completed and released for public use our first version of a turbulence spectral model that simulates turbine inflows at the Lamar Great Plains Site and incorporated it into the National Renewable Energy Laboratory (NREL) TurbSim turbulence simulation code [13]. The new model (referred to as GP_LLJ spectral model for Great Plains Low-Level Jet) simulates flow conditions associated with the large vertical shears and coherent turbulence encountered within and beneath Great Plains nocturnal LLJs similar to those shown in Figure 5. The model was constructed by using local turbulence scaling derived from measurements collected on the GE Wind 120-m tower and LLJ vertical profiles of wind speed and direction acquired with a medium range

Doppler acoustic wind profiler (SODAR) [2]. The GP_LLJ model allows the user to specify the jet height and peak wind speed (intensity) or to let the code randomly choose a jet height or wind speed based on other specified boundary conditions. It provides 12 independent sources of random variability or stochastic degrees of freedom compared to only one for the IEC NTM. The GP_LLJ model produces vertical profiles of wind speed *and* direction profiles that can be extended down to a height of 3 m AGL to simulate tower loading when the "JET" profile option is chosen. In the analysis of the Lamar data in [2] we showed that LLJs do not always break down into bursts of coherent turbulence but remain well-defined for many hours. Without this breakdown, the wind speed shear exponent often remains significantly above the IEC design criteria of 0.2. The code allows the user to simulate such conditions by requesting coherent turbulence not be added to the turbulent inflow. We have extrapolated the vertical scaling measured on the Lamar 120-m tower and believe the GP_LLJ model is applicable up to a height of 230 m AGL based on limited SODAR observations. We plan to further evaluate the model simulation performance in the 120- to 230-m height range (5- to 10-MW turbine rotors) with data from a Doppler laser wind profiler (LIDAR).

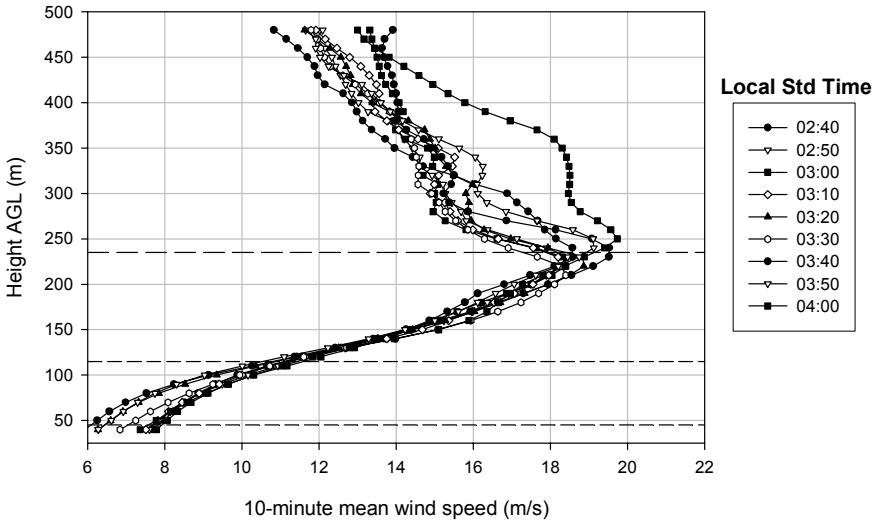


**Figure 5. Example of the observed evolution of the vertical profiles of wind speed associated with an LLJ using a Doppler SODAR.**

## Example of Comparing the TurbSim IEC NTM and GP_LLJ Spectral Model Simulations

We are in the process of comparing the collective response of the 52 static modes of the NREL virtual 5-MW Reference Turbine with inflow turbulence generated by the TurbSim Code. The physical characteristics of the NREL 5-MW Reference Turbine are summarized in Table 1. As an example, we created inflow simulations using TurbSim for two jets with their peak wind speeds at commonly observed heights of 80 and 460 m. We specified the IEC Kaimal NTM

**Table 1. NREL 5MW Reference Turbine Specifications [4]**

| Property | Specification |
|---|---|
| Rotor Diameter | 126 m |
| Rotor Orientation | Upwind |
| Control | Variable Speed, Collective Pitch |
| Hub Height | 90 m |
| Maximum Tip Speed | 80 m/s |
| Rated Wind Speed | 11.4 m/s |
| Maximum Rotor Speed | 12.1 rpm |

**Table 2. Simulated Vertical Wind Profile Characteristics**

| TurbSim Spectral Model | 80-m Jet | | | 460-m Jet | | |
|---|---|---|---|---|---|---|
| | Jet Maximum Wind Speed (m/s) | Hub (90 m) Mean Wind Speed (m/s) | Calculated Rotor Disk Shear Exponent | Jet Maximum Wind Speed (m/s) | Hub (90 m) Mean Wind Speed (m/s) | Calculated Rotor Disk Shear Exponent |
| IEC NTM "C" | *n.a.* | 11.59 | 0.200 | *n.a.* | 13.38 | 0.200 |
| GP_LLJ | 11.64 | 11.59 | 0.020 | 27.68 | 13.38 | 0.240 |

spectral model with IEC-specified "C-level" turbulence intensity (12% at a hub-height wind speed of 15 m/s). This choice is based on an analysis of the turbulence levels observed at the Lamar site. We employed the GP_LLJ spectral model with and without coherent turbulent structures. The characteristics of the resulting wind profiles across the rotor disk are listed in Table 2 and plotted in Figure 6. In the first case, the jet height of 80 m places its peak winds within the turbine rotor disk; in the second, the more intense 460-m jet maximum occurs well above the highest elevation of the rotor. For both jet heights, the mean hub-height wind speeds are identical for both spectral models, but the rotor disk speed shear profiles and corresponding exponents differ considerably. The rates of change of wind direction with height (direction shear) for the two jet heights also are quite different.

We used a 25 x 25 grid to generate 31, 10-minute full-field inflow realizations for each set of boundary conditions. The simulations used the GP_LLJ spectral model and were run with and without coherent structures requested. Each inflow realization was used to drive an MSC.ADAMS® [14] numerical model of the 5-MW reference turbine. The resulting time series of linear and angular displacements and force and moment loads from each realization were rainflow cycle-counted and equivalent displacements and fatigue damage equivalent load values calculated. Ensemble statistics were then derived for each case.

Our analysis of the results shows that, at least for the two cases studied and the two spectral models used, the IEC NTM spectral model was generally more severe but the results exhibited limited variability compared to the GP_LLJ model simulations. The exceptions are higher loads (and displacements) seen on the low-speed shaft (drivetrain), tower-top yaw bearings, and various tower locations. As expected from the large difference in the number of sources of random variability in each of the models, the GP_LLJ results often displayed wide distributions

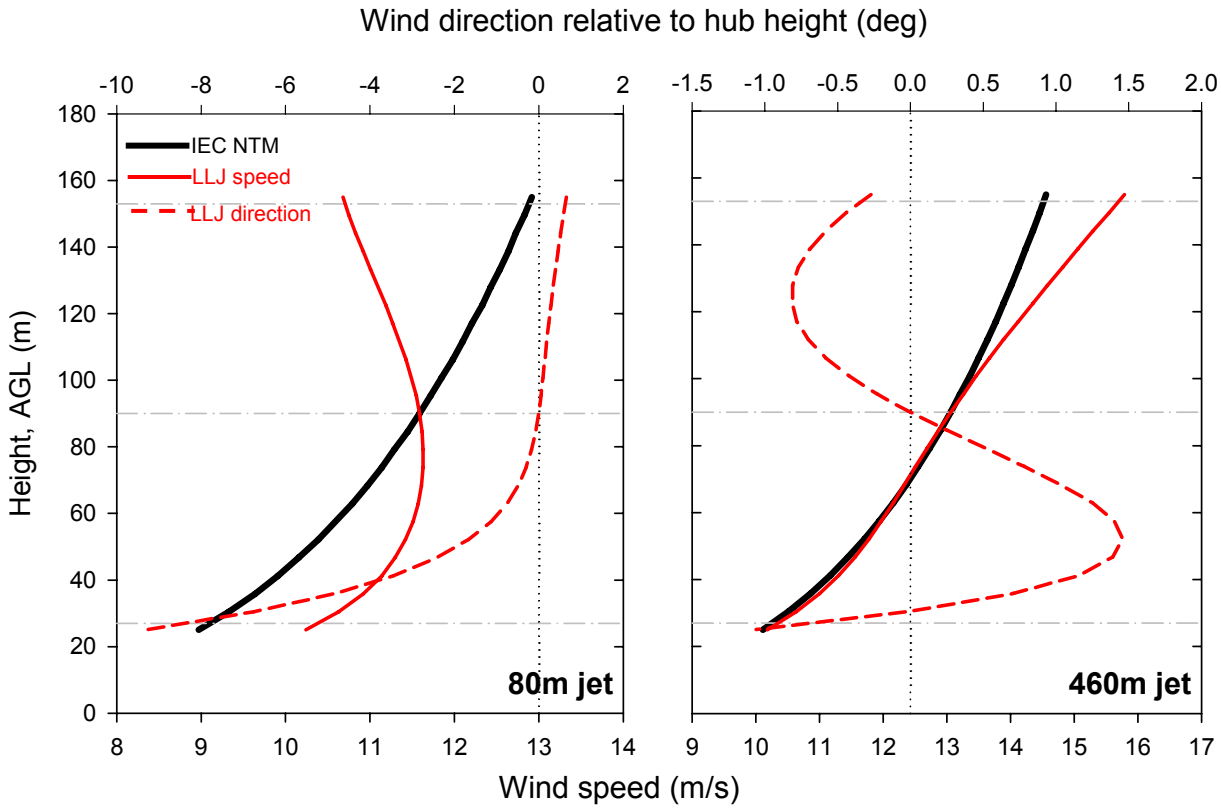


**Figure 6. Vertical wind speed and direction profiles over 5-MW turbine rotor disk for simulated 80- and 460-m LLJs.**

with positive skewness compared to the IEC NTM indicating that some of the realizations within the ensembles contained very large displacements or load excursions relative to the median or mean. Generally the means and distributions of displacements and loads resulting from the jets that included coherent turbulent structures were greater than those that did not contain coherent turbulent structures.

In Figure 7 we present a subset of equivalent displacement and load comparisons for the two jet heights and spectral models. We use the box plot graphic notation developed by Tukey [15] to present the ensemble results relative to each spectral model. In this presentation format the height of the shaded box represents the interquartile range (IQR) P25 to P75 of the distribution. We use the PXX nomenclature to indicate the XX-percentile of the ensemble distribution. The thin solid and heavier dashed lines in the box mark the distribution median (P50) and the mean (expected) value, respectively. The height of the line terminated with the "whiskers" represents the P10 to P90 range of the distribution; the distance between the black dots signifies the range between P05 to P95. The abscissa notation in Figure 7 "Jet w/o CS" refers to the box plot in which a jet had no coherent structures associated with it and "Jet w/CS" is a jet that did.

Except for the blade root out-of-plane moment loads in Figures 7-a and 7-b, medians and means and distribution widths are greater for the two jet-related simulations with the 80-m jet cases

typically having the largest relative difference to the IEC NTM. The mean values for the 460-m jet are larger than for the 80-m jet with all three models because of the higher hub-height mean wind speed (13.38. versus 11.59 m/s). The P95 tail values are also relatively larger for the GP_LLJ spectral model compared with the IEC NTM signaling the presence of large excursions within some of the individual realizations. Our analyses of observed early morning jets occurring above 200 m at the Lamar Site has shown that they are often responsible for injecting downward bursts of intense CTKE into the layer occupied by the turbine rotors. This subject will be discussed more thoroughly later. Finally, these results demonstrate that a strong jet maximum well above a turbine rotor can significantly influence the turbine response.

## Comparison of Turbulence Characteristics at the NWTC and Lamar Sites

The NWTC and GP_LLJ spectral models available in the TurbSim Code generate two diverse site-specific inflows that can be used to simulate multi-megawatt size wind turbines. We have shown previously in [2] and [9] and in Figure 1 that turbine loads reach peak values within a narrow range of the gradient Richardson number ($Ri_g$) stability parameter calculated over the depth of the turbine layer. This critical range is bounded by the *weakly stable* $Ri_g$ region of +0.000 to +0.010. We have also demonstrated the strong correlation with peak values of CTKE greater than 2 $m^2/s^2$ and turbine load excursions in [2]. In Figure 8 we compare observed hub-height peak CTKE values with $Ri_g$ for the 37-m hub height of the NWTC ART with 85-m hub of an equivalent GE 1.5 MW turbine installed at the Lamar site. In this figure we have highlighted the critical $Ri_g$ region. Many of the differences seen in the variation of peak CTKE with $Ri_g$ have to do with how this value is determined. For the ART it was calculated over a layer between 3 m and 58 m, whereas for Lamar this resides between 3 m and 116 m. We have shown in [2] that the strong peaking in maximum values of CTKE in the critical $Ri_g$ region at the NWTC is related to intense downward transport of CTKE from above the rotor disk. This process is most likely the result of KHI and breaking KH billows taking place in the lee of the Front Range of the Colorado Rocky Mountains. Some peaking takes place within the critical range at the Lamar site, but it is much less pronounced with peak values of CTKE occurring over a wider $Ri_g$ range that occurs with unstable ($Ri_g < 0$) and very stable conditions ($Ri_g > +0.25$) with the latter being more frequent. Most of the largest values of peak CTKE occur with $Ri_g$ values higher that the upper limit of the critical range. We believe this is the result of the downward injection of CTKE from jet structures located above the turbine.

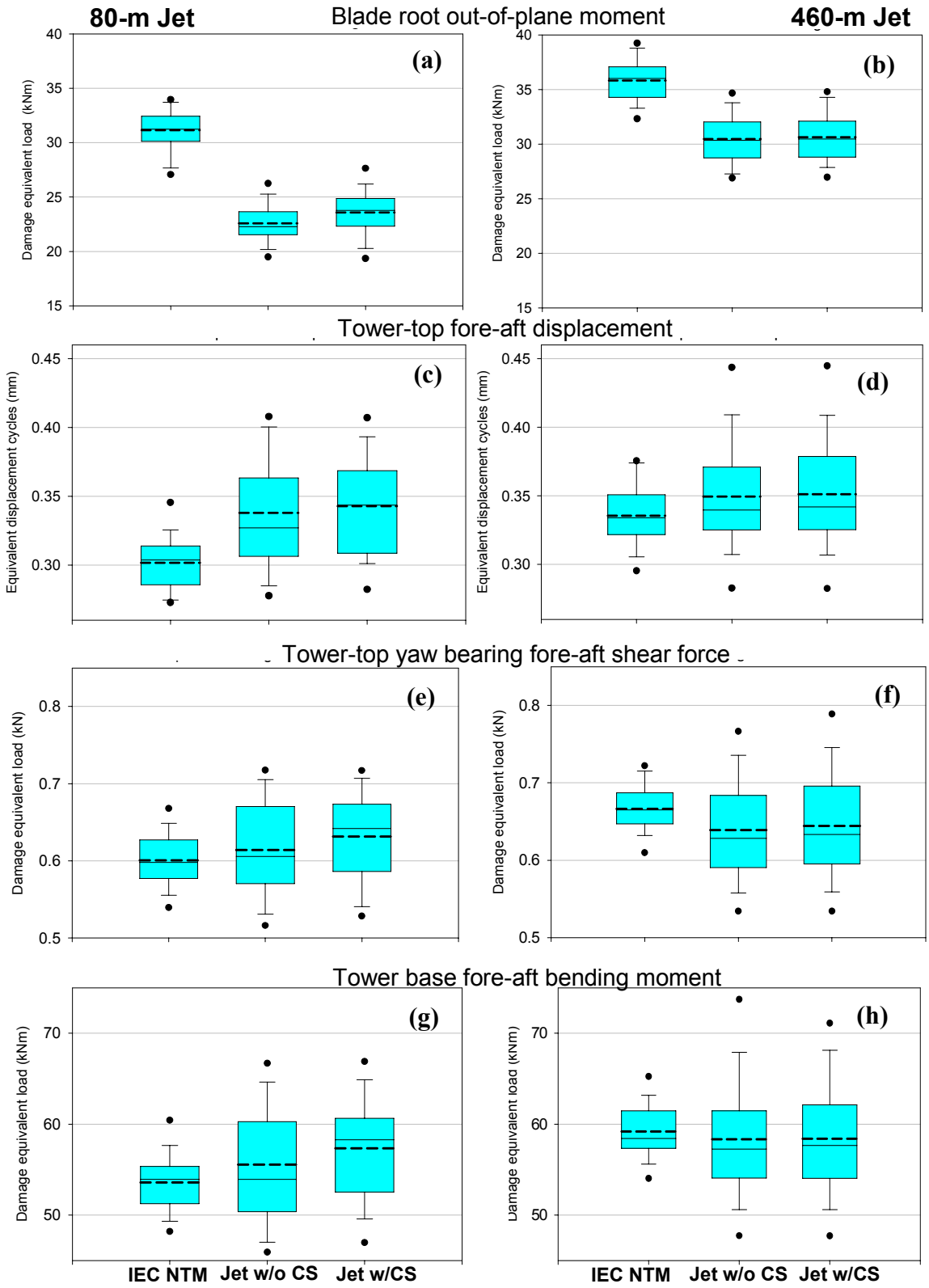


**Figure 7. Box plots of ensemble distributions of selected response variables for simulations of 5-MW reference turbine.**

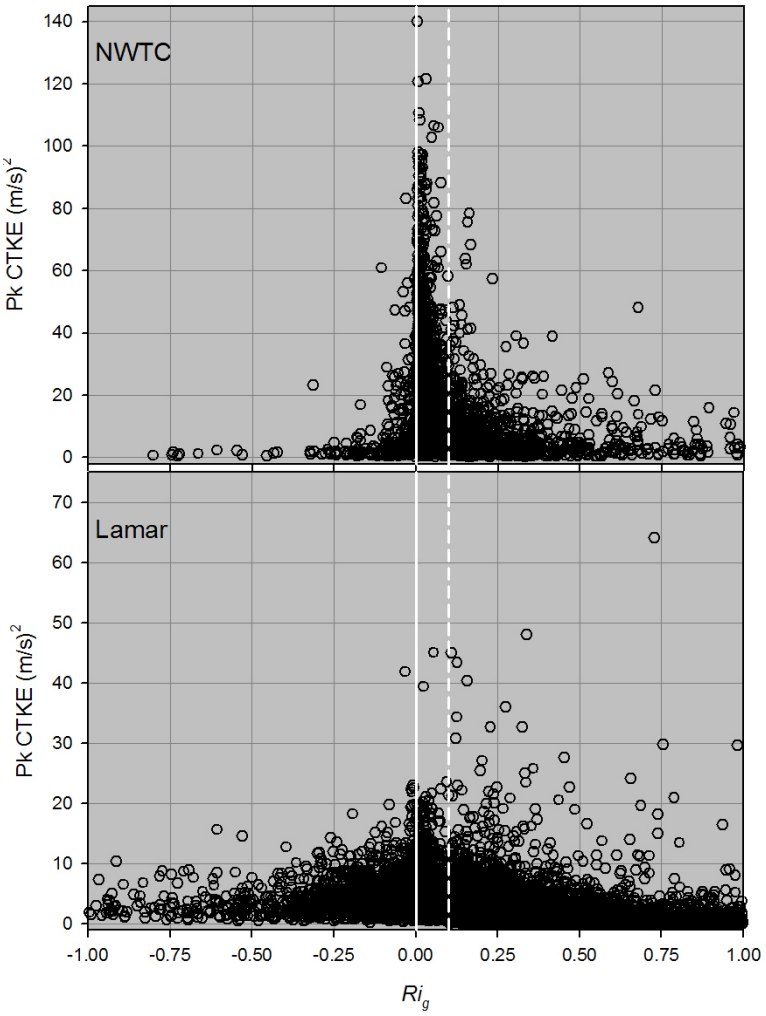


**Figure 8. Comparison of hub-height peak CTKE values versus turbine layer $Ri_g$ for the NWTC ART (37 m) and the Lamar Site (85 m).**

The downward injection of CTKE into the turbine layer occurs as the result of a net downward transport or flux of horizontal momentum. We examine in Figure 9 the observed mean vertical transport or flux of horizontal momentum, $\overline{u'w'}_D$, across the rotor disk of the ART and an equivalent GE 1.5-MW turbine as a function of $Ri_g$ at the NWTC and Lamar sites, respectively. The strongest net downward fluxes at the NWTC occur in a narrow range of $Ri_g$ (+0.000 to +0.005) which also coincides with highest root flapwise damage equivalent loads measured on the ART in Figure 1. The downward flux at Lamar occurs over a broader range of $Ri_g$, peaking in the vicinity of $Ri_g$ = +0.010. We have plotted the hub-height peak CTKE as a function of $\overline{u'w'}_D$ for the NWTC and Lamar sites in Figure 10 to see if the suspected relationship is true. Clearly the bulk of the large CTKE values at the NWTC are related to net downward momentum fluxes across the ART rotor disk and, though smaller, the same generally holds true for Lamar. Figure 11 shows that the largest values of the hub-height wind speed standard deviation or $\sigma_U$ are associated with negative or downward momentum fluxes across the rotors at both sites. The observed relationship between hub-height turbulence intensity (TI) and peak CTKE is presented in Figure 12 for both sites. There is little correlation particularly for the NWTC. The observed variations of hub-height peak CTKE and $\sigma_U$ with mean wind speed for the two sites are presented in Figures 13 and 14, respectively. Finally, the variations of vertical speed shear (expressed in terms of the shear exponent $\alpha$) across the ART disk and an equivalent Lamar GE 1.5 MW turbine rotor with $Ri_g$ and hub-height mean wind speed are presented in Figure 15.

Clearly there are marked differences between the turbine operating environments at the NWTC and those at the Lamar site. The NWTC is located in the interface between the mountains and Great Plains. This places it in the lee flows of the Front Range of the Colorado Rocky Mountains where it is subject to atmospheric processes that produce winds containing intense organized or coherent turbulent elements, high turbulence levels, and low shears over the rotor

disk of the NWTC ART. In contrast, a larger turbine installed at Lamar needs to frequently endure coherent turbulent structures that are less intense but of sufficient intensity to induce turbine responses that may occasionally become significant. At Lamar these structures occur in conjunction with much higher mean shears across the rotor disk than are typical of the NWTC.

The coherent turbulence generation process is quite different for the two sites. At the NWTC instabilities in the lee flows from the complex terrain of the mountains immediately to the west of the site produce strong winds near the surface and enhance the downward flux of turbulent momentum much of which contains intense coherent elements. The Lamar site is located on the high plains of Southeast Colorado, about 200 km east (downstream) of the Rocky Mountains. Here the primary mechanism for coherent turbulence generation is the dynamics associated with the development and life cycle of the LLJ. Intense bursts of CTKE are associated with the downward momentum fluxes accompanying instabilities that develop in the highly sheared flows beneath the LLJs. Both these contrasting environments can now be numerically simulated by the NREL TurbSim Code to assist turbine designers, wind farm planners, and operators.

## Conclusions

The Great Plains turbulence operating environment, as exemplified by the Lamar measurements, initially appears to be much less rigorous than conditions seen in and near complex terrain (such as that near the NWTC). However, a closer examination of many of the data presented in this paper underscores the challenges for designers to build large, reliable, multi-megawatt turbines, principally because of the vertical inhomogenities and instabilities associated with nocturnal boundary layer flows that are also coupled with the best wind resources.

In this paper we have demonstrated that turbulence conditions in the Great Plains can, under the right circumstances, be potentially more harmful to turbine operations than are currently being designed to. How these differences ultimately impact the productivity, reliability, and lifetime of a given turbine or turbine design will depend on the number of hours it operates in such conditions. Other than for the Lamar site, little information is available. Thus, we recommend that turbine operators undertake a more careful analysis of their operating data derived from onsite system control and data acquisition (SCADA) systems by summarizing hourly, daily, and monthly operating events and wind resources to identify trends similar to the ones we showed that may be correlated with LLJ activity and the accompanying turbulence-induced events discussed in this paper.

The NREL TurbSim Code now enables the turbine designer to replicate the Great Plains turbulence environment and conditions associated with boundary layer flows in and around complex terrain locations. It also now enables the user to test a turbine design with an extreme coherent atmospheric turbulent structure that can infrequently occur in the free atmosphere. Because of the number of sources of random variability built into these simulations, we strongly urge users to perform ensemble analysis to properly interpret the results. What the code does not do currently is to provide a more realistic turbulence environment *within* a multi-row wind park in the Great Plains. Hopefully that shortcoming can be addressed in the future.

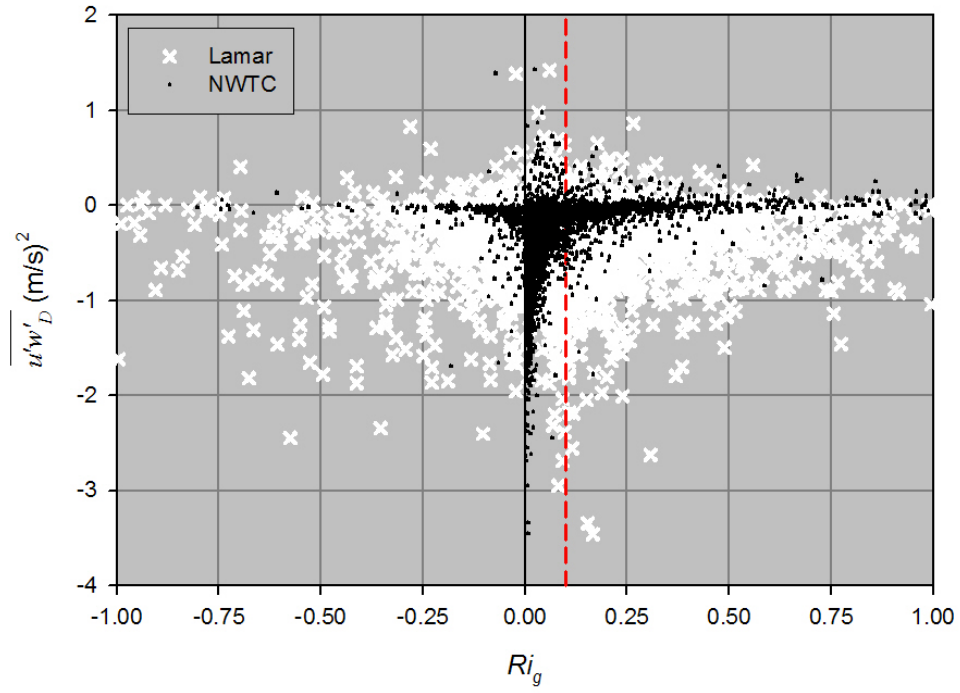


**Figure 9. Comparison of the observed mean vertical flux of horizontal momentum versus $Ri_g$ across the rotor disks of the NWTC ART and an equivalent GE 1.5-MW turbine installed at the Lamar Site.**

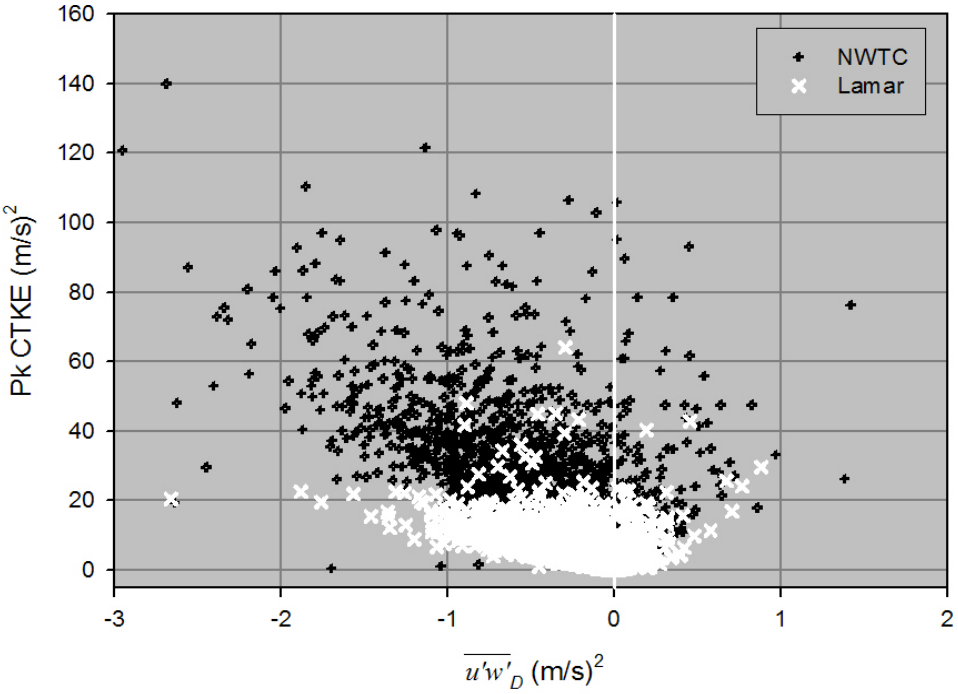


**Figure 10. Comparison of the observed hub-height peak CTKE values versus the mean vertical flux of horizontal momentum across the rotor disks of the NWTC ART and an equivalent GE 1.5-MW turbine installed at the Lamar Site.**

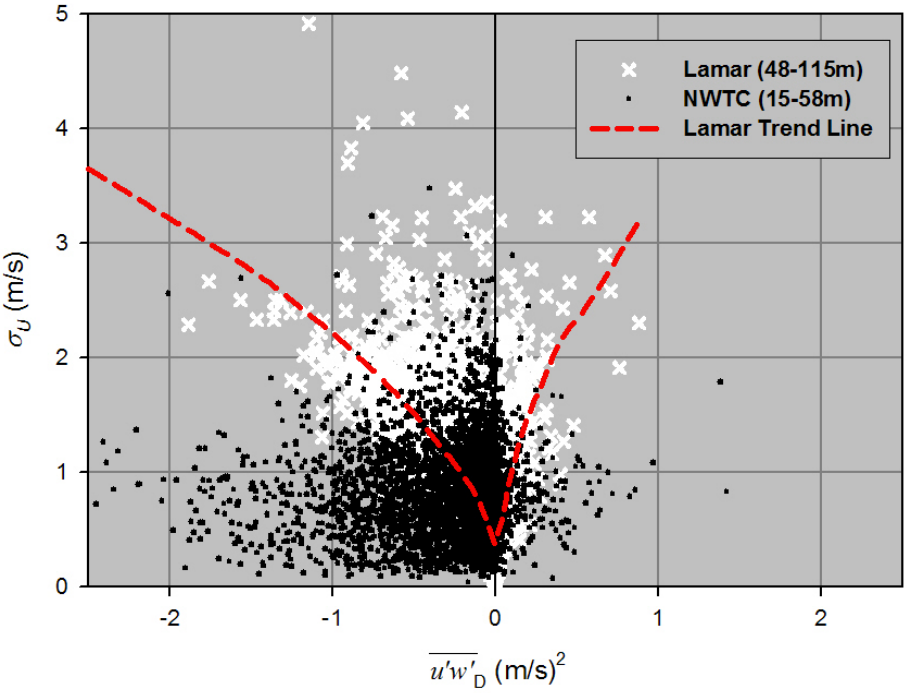


**Figure 11. Comparison of the observed hub-height $\sigma_U$ versus the mean vertical flux of horizontal momentum across the rotor disks of the NWTC ART and an equivalent GE 1.5-MW turbine installed at the Lamar Site.**

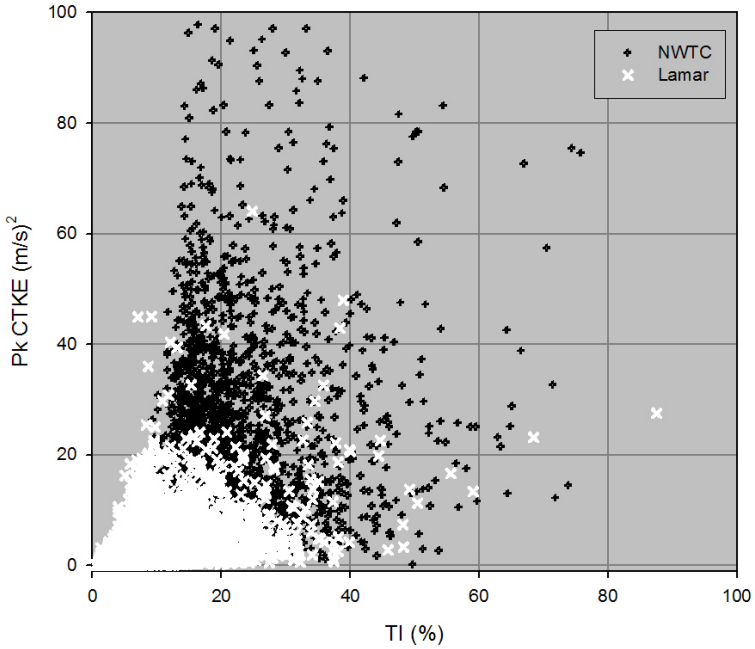


**Figure 12. Comparison of the observed variation of hub-height peak CTKE with turbulence intensity (TI) for the NWTC ART and an equivalent hub-height of a GE 1.5-MW turbine installed at the Lamar Site.**

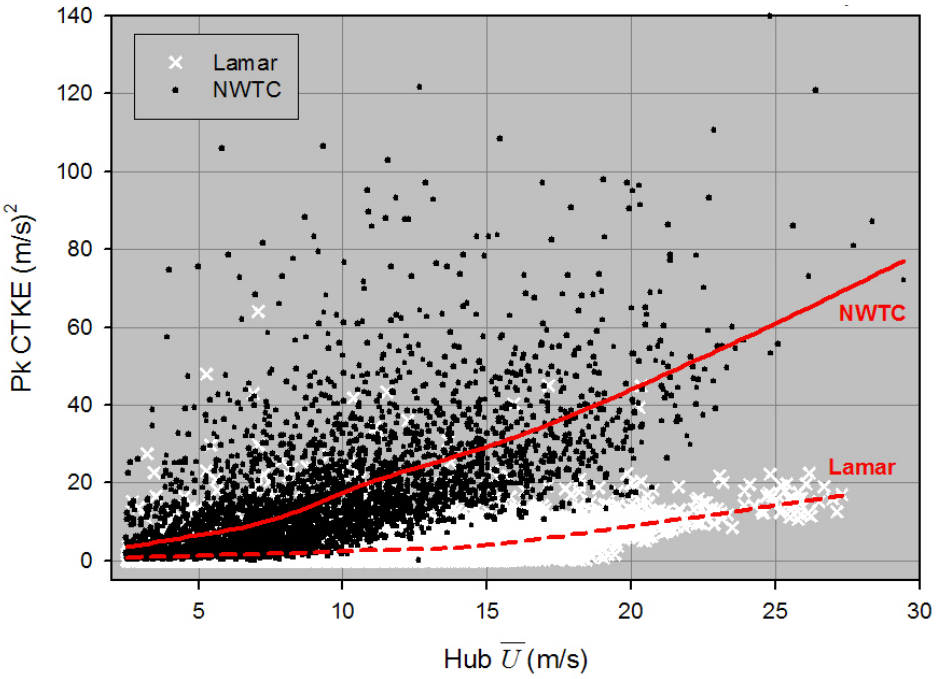


**Figure 13. Comparison of the observed variation of hub-height peak CTKE with mean wind speed for the NWTC ART and an equivalent hub-height of a GE 1.5-MW turbine installed at the Lamar Site.**

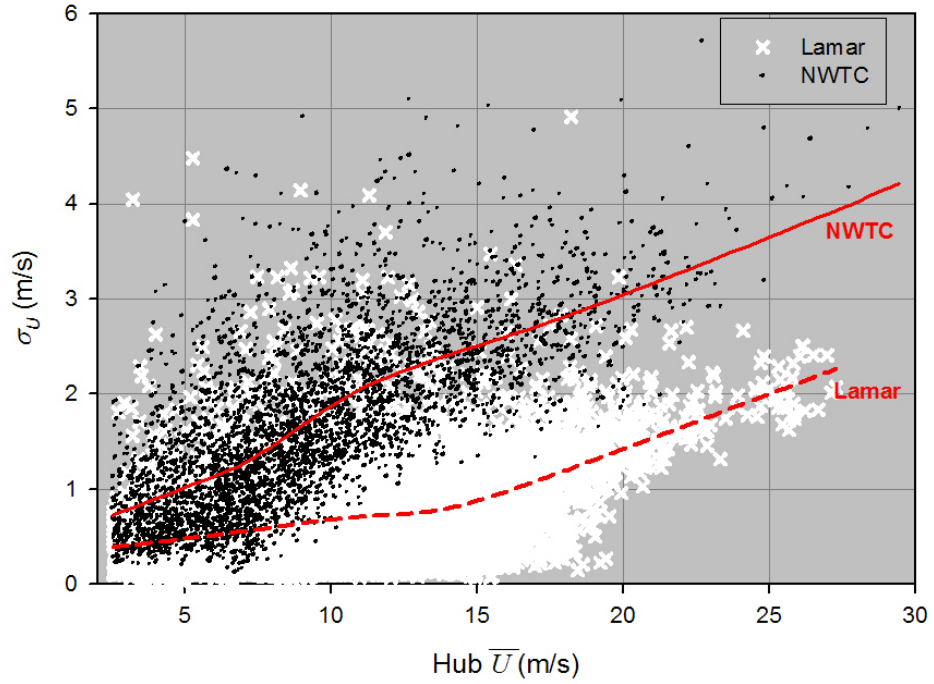


**Figure 14. Comparison of the observed variation of hub-height $\sigma_U$ with mean wind speed for the NWTC ART and at an equivalent hub-height of a GE 1.5-MW turbine installed at the Lamar Site.**

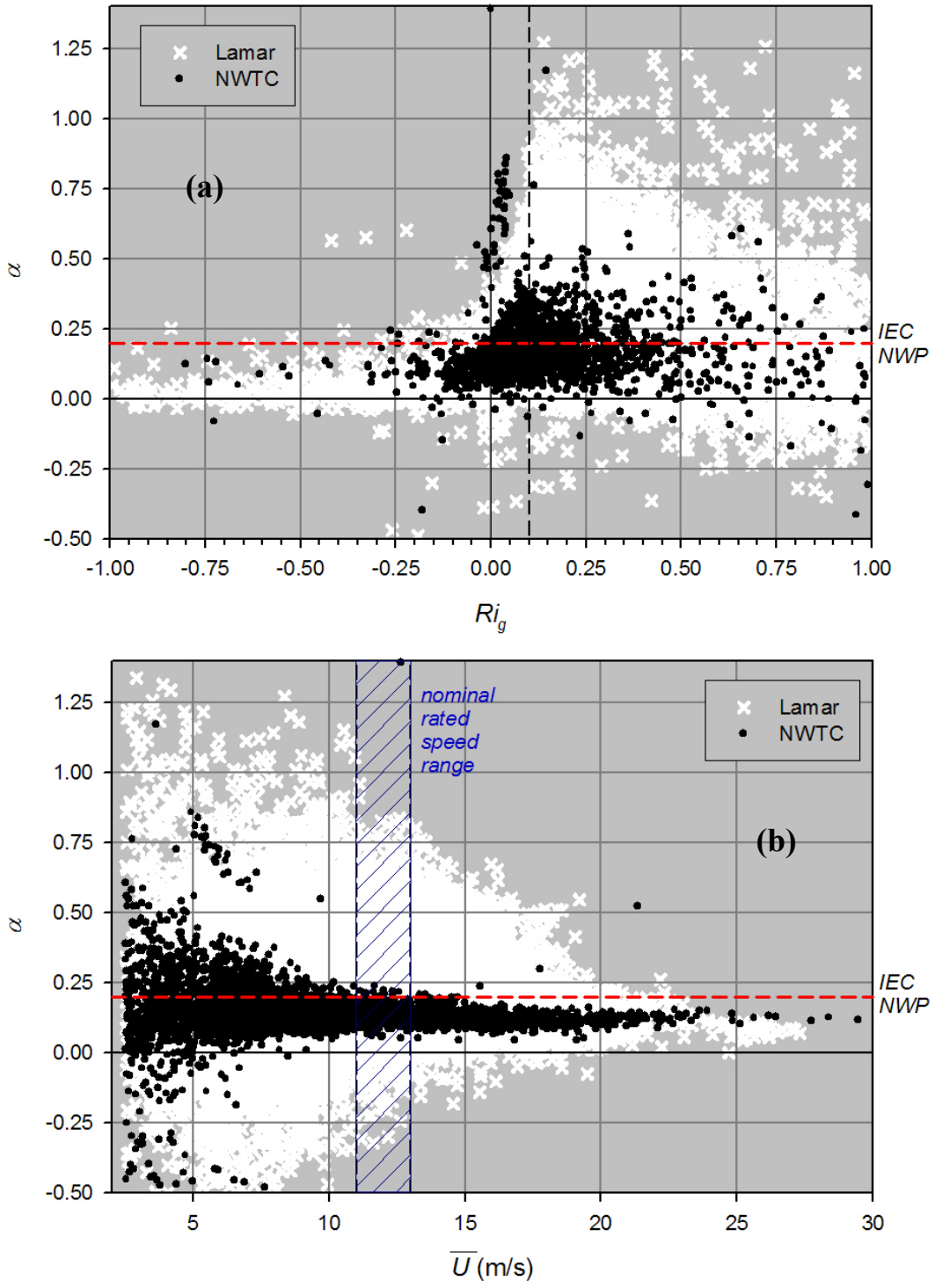


**Figure 15. Comparison of the observed rotor disk shear exponent, $\alpha$, with: (a) turbine layer $Ri_g$, and (b) hub-height mean wind speed for the NWTC ART and over an equivalent rotor disk and hub-height of a GE 1.5 MW turbine installed at the Lamar Site. The IEC Normal Wind Profile (NWP) value of 0.2 is shown as - - - - -**

## Acknowledgments

This work is supported by the U. S. Department of Energy under contract No. DE-AC36-99GO10337. We wish to thank the Office of Wind and Hydropower Technologies for supporting this effort.

## References

1. Kelley, N.D. (March 2004). "An Initial Overview of Turbulence Conditions Seen at Higher Elevations over the Western Great Plains," *Global Windpower 2004 Conference Proceedings* (CD-ROM), 28-31 March 2004, Chicago, Illinois. Washington, DC: American Wind Energy Association; Omni Press; 12 pp.; NREL Report No. CP-500-35970.

2. Kelley, N.; Shirazi, M.; Jager, D.; Wilde, S.; Adams, J.; Buhl, M.; Sullivan, P.; Patton, E. (2004) *Lamar Low-Level Jet Program – Interim Report*. National Renewable Energy Laboratory. Golden, CO. NREL Report TP-500-34593. 216 pp.

3. Malcolm, D.J.; Hansen, A.C. (August 2002). *WindPACT Turbine Rotor Design Study*. Global Energy Concepts LLC and Windward Engineering for the National Renewable Energy Laboratory. Golden, CO. NREL Report TP-500-34593, 71 pp.

4. Jonkman, J.; Butterfield, S.; Musial, W.; and Scott, G. (January 2006). "Definition of a 5 MW Reference Wind Turbine for Offshore System Development," Golden, CO: National Renewable Energy Laboratory. NREL Report TP-500-38060 (to be published).

5. International Electrotechnical Commission. (2005). *Wind Turbines-Part 1: Design Standards.* 61400-1, 3ed. http://www.iec.ch.

6. Kaimal, J.C.; Wyngaard, J.C.; Izumi, Y.; Cote, O.R. (1972). "Spectral Characteristics of Surface-Layer Turbulence." *Quarterly Journal of the Royal Meteorological Society* (21), pp. 563−598.

7. Mann, J. (1994). "The Spatial Structure of Neutral Atmospheric Surface-Layer Turbulence." *Journal of Fluid Mechanics* (273), pp. 41−168.

8. Mann, J. (1998). "Wind Field Simulation." *Journal of Probabilistic Engineering Mechanics* (13), pp. 269−282.

9. Kelley, N.D.; Jonkman, B.J.; Scott, G.N.; Bialasiewicz, J.T.; Redmond, L.S. (May 2005). "The Impact of Coherent Turbulence on Wind Turbine Aeroelastic Response and Its Simulation," *Windpower 2005 Conference Proceedings* (CD-ROM), 15-18 May 2005, Denver, CO. Washington, DC: American Wind Energy Association; Omni Press; 19 pp.; NREL Report CP-500-38074.

10. Smith, K.; Randall, G.; Malcolm, D.; Kelley, N.; Smith, B. (June 2002). "Evaluation of Wind Shear Patterns at Midwest Wind Energy Facilities." *Windpower 2002 Conference Proceedings*, 2−5 June 2002, Portland, OR. Washington, DC: American Wind Energy Association; 16 pp.

11. Mitchell, M.K.; Arritt, R.W.; Labas, K. (September 1995). "An Hourly Climatology of the Summertime Great Plains Low-Level Jet Using Wind Profiler Observations." *Weather Forecasting* (10), pp. 576−591.

12. Whiteman, C.D.; Bian, X.; Zhong, S. (October 1997). "Low-Level Jet Climatology from Enhanced Rawinsonde Observations at a Site in the Southern Great Plains." *Journal of Applied Meteorology* (36), pp. 1363−1376.

13. Kelley, N.D.; Jonkman, B.J. (April 2006). "Overview of the TurbSim Stochastic Inflow Turbulence Simulator – Version 1.10." Golden, CO: National Renewable Energy Laboratory. NREL Report TP-500-39796. It is available at http://wind.nrel.gov/designcodes/preprocessors/turbsim

14. MSC. Software Corporation. *ADAMS/Solver Task Documentation Kit. Version 12.0* Santa Ana, CA: MSC. Software Corporation.

15. Tukey, J.W. (1977). *Exploratory Data Analysis.* Reading, MA: Addison-Wesley.

# REPORT DOCUMENTATION PAGE

*Form Approved*
*OMB No. 0704-0188*



**PLEASE DO NOT RETURN YOUR FORM TO THE ABOVE ORGANIZATION.**

| 1. REPORT DATE *(DD-MM-YYYY)* | 2. REPORT TYPE | 3. DATES COVERED *(From - To)* |
|---|---|---|
| December 2006 | Conference paper | |

**4. TITLE AND SUBTITLE**
The Great Plains Turbulence Environment: Its Origins, Impact, and Simulation

**5a. CONTRACT NUMBER**
DE-AC36-99-GO10337

**5b. GRANT NUMBER**

**5c. PROGRAM ELEMENT NUMBER**

**6. AUTHOR(S)**
N.D. Kelley, B.J. Jonkman, and G.N. Scott

**5d. PROJECT NUMBER**
NREL/CP-500-40176

**5e. TASK NUMBER**
WER6.2104

**5f. WORK UNIT NUMBER**

**7. PERFORMING ORGANIZATION NAME(S) AND ADDRESS(ES)**
National Renewable Energy Laboratory
1617 Cole Blvd.
Golden, CO 80401-3393

**8. PERFORMING ORGANIZATION REPORT NUMBER**
NREL/CP-500-40176

**9. SPONSORING/MONITORING AGENCY NAME(S) AND ADDRESS(ES)**

**10. SPONSOR/MONITOR'S ACRONYM(S)**
NREL

**11. SPONSORING/MONITORING AGENCY REPORT NUMBER**

**12. DISTRIBUTION AVAILABILITY STATEMENT**
National Technical Information Service
U.S. Department of Commerce
5285 Port Royal Road
Springfield, VA 22161

**13. SUPPLEMENTARY NOTES**

**14. ABSTRACT** *(Maximum 200 Words)*

This paper summarizes the known impacts of nocturnal turbulence on wind turbine performance and operations and discusses NREL's progress in numerically simulated coherent inflow turbulent conditions generated by atmospheric instabilities that are frequently assiciated with a Great Plains nocturnal low-level jet stream.

**15. SUBJECT TERMS**
wind energy; wind plant development; Great Plains turbulence; wind resources; wind turbine siting

| 16. SECURITY CLASSIFICATION OF: | | | 17. LIMITATION OF ABSTRACT | 18. NUMBER OF PAGES | 19a. NAME OF RESPONSIBLE PERSON |
|---|---|---|---|---|---|
| a. REPORT | b. ABSTRACT | c. THIS PAGE | | | 19b. TELEPHONE NUMBER (*Include area code*) |
| Unclassified | Unclassified | Unclassified | UL | | |

**Standard Form 298** (Rev. 8/98)
Prescribed by ANSI Std. Z39.18